Journal of Nuclear Materials 430 (2012) 190–193

Contents lists available at SciVerse ScienceDirect

Journal of Nuclear Materials

journal homepage: www.elsevier.com/locate/jnucmat

Influence of oversized elements (Hf, Zr, Ti and Nb) on the thermal stability of vacancies in type 316L stainless steels

A. Yabuuchi *, M. Maekawa, A. Kawasuso

Advanced Science Research Center, Japan Atomic Energy Agency, 1233 Watanuki, Takasaki, Gunma 370-1292, Japan

ARTICLE INFO

Article history:
Received 27 April 2012
Accepted 3 July 2012
Available online 11 July 2012

ABSTRACT

To reveal the influence of oversized elements on the thermal stability of vacancies in type 316L stainless steels, vacancy recovery processes were investigated by means of positron annihilation spectroscopy. Although vacancies in additive-free 316L stainless steels were mobile at 300 °C, which is a typical nuclear reactor operating temperature, vacancies in oversized elements doped 316L were stable up to 300–350 °C. This result indicates that oversized elements stabilize vacancies in stainless steels. Stability of vacancies inhibits the radiation-induced grain boundary segregation and may also lead to suppression of high-temperature water stress corrosion cracking that is observed in nuclear materials.

1. Introduction

Low-carbon stainless steels are commonly used as nuclear reactor materials. Despite their strong resistance to sensitisation, stress corrosion cracking (SCC) in high-temperature water environments has been reported. It has recently been hypothesized that SCC crack propagation is induced by aggregation of vacancies to grain boundaries at crack tips [1–3]. We use positron annihilation spectroscopy to investigate this phenomenon finding that monovacancies generate around SCC cracks [4–6] and these monovacancies are mobile at approximately 300 °C, which is a typical nuclear reactor operating temperature [7]. We therefore assume that the high-temperature water SCC can be controlled by passivating monovacancies at the nuclear reactor operating temperature. It has been reported that radiation-induced grain boundary segregation is inhibited by doping oversized elements, such as Hf and Zr, to stainless steels [8–13]. This effect is thought to be due to the binding of mobile vacancies to oversized elements. As a result, the flow of vacancies to grain boundaries is decreased and the grain boundary segregation caused by inverse Kirkendall effect is suppressed. In the present study, solute-vacancy binding effect was examined for type 316L stainless steels modified with oversized elements by means of positron annihilation spectroscopy.

2. Experimental

Alloy ingots of 316L–0.5 at%Hf, 316L–0.5 at%Zr, 316L–0.5 at%Ti, and 316L–0.5 at%Nb were prepared by melting commercially available type 316L stainless steels (Fe: 66.17 at%; Cr: 18.63 at%; Ni: 11.49 at%; Si: 1.25 at%; Mo: 1.19 at%; Mn: 1.18 at%; P: 0.05 at%; C: 0.04 at%) and Hf (Zr, Ti, Nb) in a vacuum arc melting furnace. From these ingots, $10 \times 10 \times 1.5$ mm^3 volume specimens were cut out. To suppress chromium carbide precipitation, each specimen was annealed at 1150 °C for 2 h in vacuum and subsequently quenched in ice water. To serve as a reference, unaltered 316L specimens were also annealed and water-quenched at the same temperature. All specimens were then irradiated with 2 MeV electrons at approximately 50 °C using a Cockcroft–Walton type accelerator in Takasaki Advanced Radiation Research Institute, Japan Atomic Energy Agency. A dose rate was 4.9×10^{13} e$^-$/cm^2 s, corresponding to a damage rate of 1.5×10^{-9} dpa/s, assuming a threshold displacement energy of 40 eV and using the displacement cross section given by Oen [14]. The irradiation was carried out up to a total dose of 1.5×10^{18} e$^-$/cm^2, corresponding to a total damage level of 4.5×10^{-5} dpa. These specimens were then isochronally annealed in vacuum with a temperature step of 50 °C for a duration of 15 min. After each annealing step, the specimens were quenched in ice water.

Positron annihilation measurements were conducted using a positron source (^{22}NaCl, 700 kBq) deposited onto a titanium foil (thickness: 5 μm) and a fast-fast spectrometer with a time resolution of 245 ps (full width at half-maximum). After source and background corrections, the lifetime spectra were decomposed into two exponential terms:

$$L(t) = (I_1/\tau_1)\exp(-t/\tau_1) + (I_2/\tau_2)\exp(-t/\tau_2)$$

where τ_i and I_i are the ith lifetime component and its intensity. The total intensity of the two components is unity ($I_1 + I_2 = 100\%$). Based on the two-state trapping model, τ_2 is related to the positron

* Corresponding author. Address: Research Organization for the 21st Century, Osaka Prefecture University, 1-1 Gakuen-cho, Naka-ku, Sakai, Osaka 599-8531, Japan. Tel./fax: +81 72 254 9812.
E-mail address: yabuuchi.atsushi@21c.osakafu-u.ac.jp (A. Yabuuchi).

0022-3115/$ - see front matter © 2012 Elsevier B.V. All rights reserved.
http://dx.doi.org/10.1016/j.jnucmat.2012.07.005

lifetime at vacancies ($\tau_2 = \tau_v$). The positron trapping rate to vacancies is given by $\kappa = (I_2/I_1)(\tau_b^{-1} - \tau_2^{-1})$, where τ_b and τ_v are positron lifetimes for bulk and vacancies. The first lifetime is given by $\tau_1^{TM} = 1/(\tau_b^{-1} + \kappa)$. The validity of the two-state trapping model is confirmed by τ_1 and τ_1^{TM} agreement.

To analyze electron momentum distribution, coincidence Doppler broadening (CDB) measurements were performed using the same positron source and two high-purity germanium detectors.

3. Results and discussion

3.1. As-irradiated state

The reference specimen (annealed 316L alloy) had a one lifetime value of 105 ps. This is attributed to the bulk positron lifetime [15–18]. Thus, before irradiation, the vacancy concentration was under the detection limit ($<10^{-7}$). Fig. 1 shows the positron lifetimes (τ_1 and τ_2) and intensity (I_2) obtained for each specimen after irradiation. In all specimens, τ_1 and τ_1^{TM} agree with each other, suggesting the validity of the two-component trapping model. For the additive-free 316L specimen, the vacancy-related positron lifetime was $\tau_2 = 180$ ps, with $I_2 = 69\%$. This positron lifetime is close to that of monovacancy in pure Fe [15,16]. For the additive-modified 316L specimens, the vacancy-related lifetimes are $\tau_2 = 161 \sim 165$ ps. The reduced lifetimes indicate that irradiation-induced monovacancies are trapped by oversized elements, decreasing the effective vacancy volumes [19,20]. Although the linear size factor [21] of additive elements in 316L alloy decreases in order corresponding to Hf (43.12%) → Zr (36.83%) → Nb (17.56%) → Ti (11.15%), the second intensity (I_2) decreases in the following order: 316L–Hf (66%) → 316L–Zr (62%) → 316L–Ti (54%) → 316L–Nb (37%). This trend corresponds well with the trend of the inhibitory effect of radiation-induced grain boundary segregation due to the addition of each oversized element [8], which is likely caused by the difference in strengths of interactions between vacancies and additive elements. In a theoretical study of solute–vacancy binding energy of aluminum [22], it was reported that not only solute size but also strength of chemical bonding between solute atoms and matrix atoms is a factor in controlling binding energy. For this reason, it is understandable that the I_2 order is not the same as the size factor order.

That the I_2 value of the additive-free 316L alloy after irradiation was the largest can be interpreted as follows. In this study, the 316L alloys modified with oversized elements were prepared by vacuum melting, but the additive-free 316L alloy was not. As an analogous example, vacuum melting in steels decreases carbon concentration. Additionally, it has been reported that there are strong interactions between vacancies and carbon atoms in pure Fe [23,16]. It is considered that this result reflects the differences in carbon concentrations in these specimens. On the other hand, all the oversized additives used in this study are carbide formers. It is also known that positrons detect carbide precipitation [24], because carbides have a large lattice mismatch with the austenite matrix. In addition, calculated lattice constants of the HfC, ZrC, TiC and NbC are 27%, 29%, 19% and 23% larger, respectively, than that of the matrix have been reported [25]. However, as described in Section 3.2, positron trapping rates for all additive-modified 316L specimens decrease to nearly zero after annealing at 500 °C. This fact indicates that carbides are not formed in these as-irradiated specimens, i.e., carbon atoms are not consumed by carbide formation.

Fig. 2 shows the CDB ratio spectra for the as-irradiated specimens, normalized to the momentum distribution of the well-annealed pure Fe. CDB spectra also indicate that vacancies are included in all specimens after irradiation. However, in the high-momentum region reflecting the elemental difference, no remarkable change is observed in the shape of each spectrum. Although the CDB spectra of pure Hf, Zr, Ti and Nb were also measured as reference spectra, the shape of each spectrum was similar in the high-momentum region. Thus, in the CDB spectra of Fig. 2, it is considered that the differences of the additive elements do not appear as a change in spectrum shape.

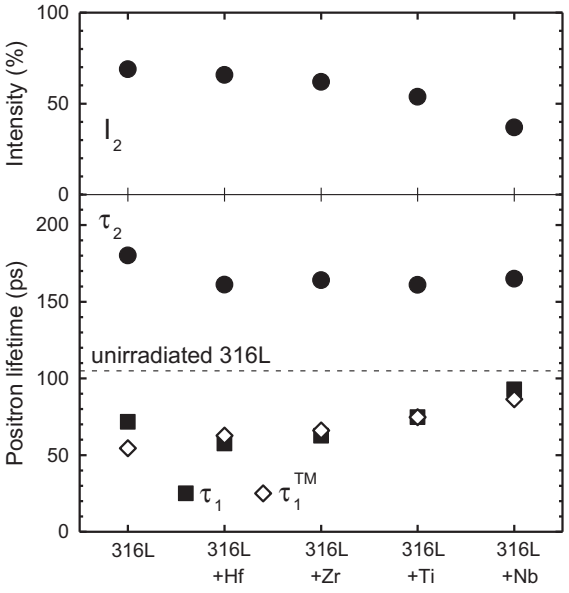

Fig. 1. Positron lifetimes (τ_1 and τ_2) and intensity (I_2) obtained for each specimen after electron irradiation. The calculated lifetime τ_1^{TM} is also plotted. The positron lifetime obtained for unirradiated 316L is depicted by a horizontal dashed line. Error bars are smaller than the sizes of the symbols.

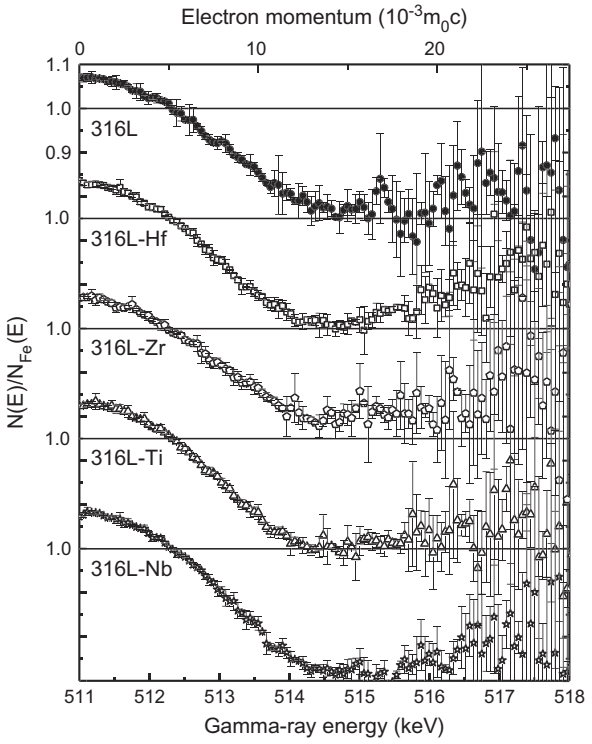

Fig. 2. Electron momentum distributions (CDB spectra) obtained for each specimen after electron irradiation. All spectra are normalized to the electron momentum distribution of well-annealed pure Fe.

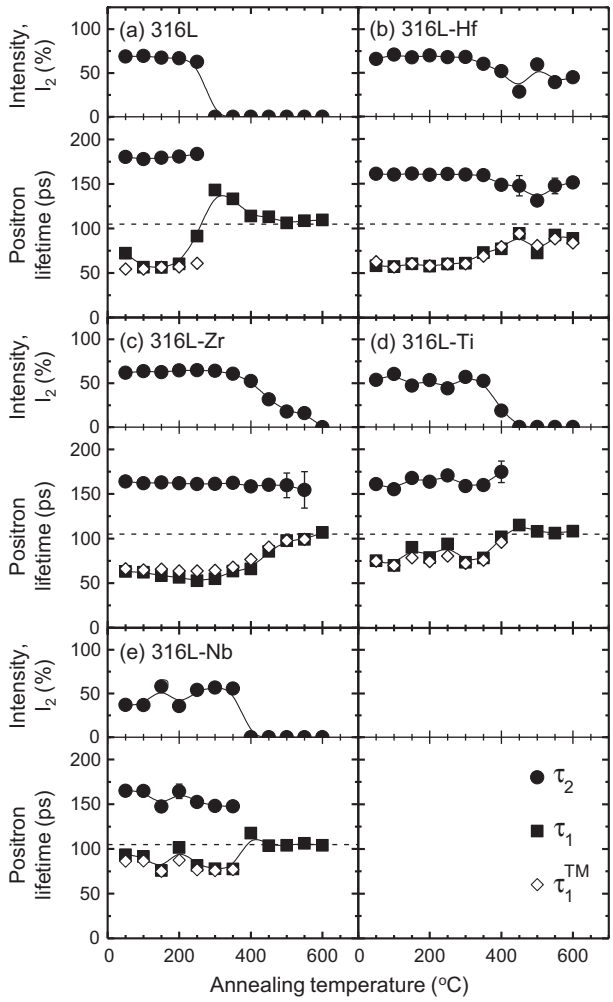

Fig. 3. Positron lifetimes (τ_1 and τ_2) and intensity (I_2) obtained for each specimen after electron irradiation as a function of annealing temperature. The positron lifetime obtained for unirradiated 316L is depicted by a horizontal dashed line. Error bars of τ_1 are smaller than the sizes of the symbols.

3.2. Annealing behavior

Fig. 3 shows the isochronal annealing behavior of positron lifetimes (τ_1 and τ_2) and intensities (I_2) after irradiation. Again, τ_1 and τ_1^{TM} agree each other, reinforcing the validity of the analysis using a two-component trapping model. In all specimens, the vacancy-related lifetimes (τ_2) do not increase during annealing. This suggests that vacancy clustering is not a major annealing process. Except for the 316L–Hf alloy, the second lifetime components (τ_2) related to vacancy defects eventually disappear. In the case of the 316L–Hf alloy, the τ_2 once decreases to 131 ps, and re-increases at above 500 °C. The positron lifetime of 131 ps is attributed to dislocation-related defects, i.e., dislocations or vacancies on the edge dislocation line [26,27]. Hafnium has been recognized as the highest element of carbide forming ability among the oversized elements used in this study. In Neutron irradiated type 316 stainless steel, it has been reported that fine hafnium carbide (HfC) precipitates are formed at 500–600 °C [28]. Therefore, the annealing behavior of the 316L–Hf alloy may be explained as follows. After annealing at 500 °C, positrons are trapped at misfit dislocation related defects formed by the HfC precipitates. The further annealing leads to growth of HfC precipitates, and then positrons are trapped at strain-induced vacancies. The formation of strain-induced vacancy due to a precipitation of second phase has also been reported in a palladium hydrogenation-dehydrogenation process [29].

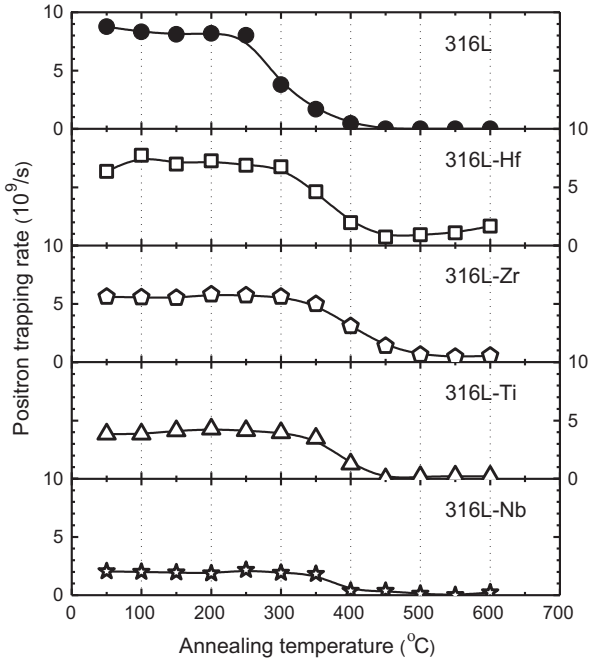

Fig. 4. Positron trapping rates (κ) obtained for each specimen after electron irradiation as a function of annealing temperature.

Fig. 4 shows the positron trapping rates, which are proportional to vacancy concentration, obtained for each specimen after irradiation as a function of annealing temperature. Focusing on the annealing process, the positron trapping rate of the additive-free 316L specimen decreases drastically at 300 °C. The recovery temperature seems to shift to 350–400 °C by adding oversized elements, indicating that these oversized elements stabilize the vacancies in stainless steels. The recovery temperature of vacancies seems to be similar between each additive-modified 316L specimen, suggesting that there is little difference in binding energy between vacancy and additive atom. The only difference is that the κ of the 316L–Hf alloy is re-increased at above 500 °C. This re-increase is attributed to the precipitation of HfC mentioned above.

On the other hand, the value of κ after irradiation changes drastically with additive elements. Furthermore, the additive-free 316L specimen has its largest κ after irradiation, even though the recovery temperature of the additive-free 316L specimen is lower than that of the additive-modified 316L specimens. A similar phenomenon was also observed in a past positron annihilation study of electron-irradiated Fe-based dilute binary alloys [30]. In that study, the recovery temperature of vacancies in an Fe–C dilute alloy were lower than those of an Fe–Si dilute alloy. It has further been reported that the vacancy-related intensity I_2 of Fe–C after irradiation is larger than that of Fe–Si. These results may be attributed to differences in vacancy capture cross sections for each additive element.

4. Conclusions

We utilized positron annihilation spectroscopy to examine thermal stability of vacancies in type 316L stainless steels modified with oversized elements. The results show that the oversized elements stabilize vacancies, suppressing the flow of vacancies to grain boundaries. Eventually, the stabilized vacancies annihilate by recombining with interstitial atoms during heavy irradiation. The decrease in the flow of vacancies inhibits radiation-induced grain boundary segregation and may also lead to suppression of high-temperature water SCC crack propagation observed in non-sensitized stainless steels.

Acknowledgements

This study was supported by the Ministry of Education, Culture, Sports, Science and Technology of Japan (MEXT) Grant-in-Aid for Young Scientists (B), No. 22760682, 2010.

References

[1] R.W. Staehle, in: Proceedings of the International Conference on Water Chemistry of Nuclear Reactor Systems, Jeju Island, Korea, 2006.
[2] K. Arioka, T. Yamada, T. Terachi, T. Miyamoto, Corrosion 64 (2008) 691.
[3] K. Arioka, T. Miyamoto, T. Yamada, T. Terachi, Corrosion 66 (2010) 015008.
[4] M. Maekawa, A. Kawasuso, T. Hirade, Y. Miwa, Mater. Sci. Forum 607 (2009) 266.
[5] M. Maekawa, A. Yabuuchi, A. Kawasuso, J. Phys.: Conf. Ser. 225 (2010) 012033.
[6] A. Yabuuchi, M. Maekawa, A. Kawasuso, J. Phys.: Conf. Ser. 262 (2011) 012067.
[7] A. Yabuuchi, M. Maekawa, A. Kawasuso, J. Nucl. Mater. 419 (2011) 9.
[8] T. Kato, H. Takahashi, M. Izumiya, J. Nucl. Mater. 189 (1992) 167.
[9] N. Sakaguchi, S. Watanabe, H. Takahashi, Nucl. Instrum. Methods Phys. Res. B 153 (1999) 142.
[10] S. Kasahara, K. Nakata, J. Kuniya, H. Takahashi, J. Electron Microscopy 48 (1999) 431.
[11] L. Fournier, B.H. Sencer, G.S. Was, E.P. Simonen, S.M. Bruemmer, J. Nucl. Mater. 321 (2003) 192.
[12] M.J. Hackett, J.T. Busby, G.S. Was, Metall. Mater. Trans. A 39A (2008) 218.
[13] M.J. Hackett, J.T. Busby, M.K. Miller, G.S. Was, J. Nucl. Mater. 389 (2009) 265.
[14] O.S. Oen, Cross Sections for Atomic Displacements in Solids by Fast Electrons, Report ORNL-4897, Oak Ridge National Laboratory, 1973.
[15] P. Hautojärvi, T. Judin, A. Vehanen, J. Yli-Kauppila, Solid State Commun. 29 (1979) 855.
[16] A. Vehanen, P. Hautojärvi, J. Johansson, J. Yli-Kauppila, P. Moser, Phys. Rev. B 25 (1982) 762.
[17] H.-E. Schaefer, R. Würschum, Phys. Lett. A 119 (1987) 370.
[18] H.-E. Schaefer, R. Würschum, R. Birringer, H. Gleiter, Phys. Rev. B 38 (1988) 9545.
[19] E. Kuramoto, H. Abe, M. Takenaka, F. Hori, Y. Kamimura, M. Kimura, K. Ueno, J. Nucl. Mater. 239 (1996) 54.
[20] A. Yabuuchi, Y. Yamamoto, J. Ohira, K. Sugita, M. Mizuno, H. Araki, Y. Shirai, J. Phys.: Conf. Ser. 191 (2009) 012019.
[21] T. Kato, H. Takahashi, M. Izumiya, Mater. Trans. JIM 32 (1991) 921.
[22] C. Wolverton, Acta Mater. 55 (2007) 5867.
[23] P. Hautojärvi, J. Johansson, A. Vehanen, J. Yli-Kauppila, Phys. Rev. Lett. 44 (1980) 1326.
[24] J. Arunkumar, S. Abhaya, R. Rajaraman, G. Amarendra, K.G.M. Nair, C.S. Sundar, B. Raj, J. Nucl. Mater. 384 (2009) 245.
[25] W.S. Jung, S.H. Chung, Modell. Simul. Mater. Sci. Eng. 18 (2010) 075008.
[26] Y. Kamimura, T. Tsutsumi, E. Kuramoto, Phys. Rev. B 52 (1995) 879.
[27] Y. Kamimura, T. Tsutsumi, E. Kuramoto, J. Phys. Soc. Jpn. 66 (1997) 3090.
[28] S. Ohnuki, S. Yamashita, H. Takahashi, T. Kato, in: Effects of Radiation on Materials: 19th International Symposium, ASTM STP 1366, ASTM, West Conshochoken, PA, 2000, p. 756.
[29] K. Sakaki, M. Mizuno, H. Araki, Y. Shirai, J. Alloys Compd. 414 (2006) 204.
[30] Y. Nagai, K. Takadate, Z. Tang, H. Ohkubo, H. Sunaga, H. Takizawa, M. Hasegawa, Phys. Rev. B 67 (2003) 224202.